

Effects of the Al content on pore structures of porous Ti_3AlC_2 ceramics by reactive synthesis

Junsheng Yang, Cuijiao Liao, Jiefeng Wang, Yao Jiang, Yuehui He*

State Key Laboratory for Powder Metallurgy, Central South University, Changsha 410083, China

Received 9 July 2013; received in revised form 28 August 2013; accepted 2 September 2013

Available online 7 September 2013

Abstract

Porous Ti_3AlC_2 ceramics were fabricated through the reactive synthesis method with TiH_2 , Al and graphite powders. The effect of Al content on phase constitution, volume expansion, pore size and permeability were studied systematically. The experimental results showed that the Al content has a great affect on the properties and pore structures of porous Ti_3AlC_2 ceramics. When Al molar ratio was less than 1.2, the volume expansion ratio, the amount of Ti_3AlC_2 and porosity were improved with the increase in Al content. In contrary, these parameters of the porous Ti_3AlC_2 decreased while the Al molar ratio was more than 1.2. However, it was interesting to notice that the evolution of pore size and permeability was opposite to that of porosity. The fundamental reasons behind these phenomena have been explored. The pore structure forming mechanism by active sintering synthesis has also been proposed.

© 2013 Elsevier Ltd and Techna Group S.r.l. All rights reserved.

Keywords: A. Sintering; A. Solid state reaction; B. Porosity; D. Carbides; Pore forming mechanism

1. Introduction

Layered ternary ceramic Ti_3AlC_2 is a new member of ternary carbides (M_3AX_2 , where M is a transition metal, A is a group A element, and X is either C or N). It has been attracted with increasing attention owing to its unique combinative properties of both ceramics and metals. On the one hand, they are thermally and electrically conductive [1], easy to machine with conventional tools [2], and resistant to thermal shock [3]; on the other hand, they have high strength, high melting points, thermal stabilities [4] and excellent corrosion resistance in acid/alkali solution [5,6].

The current inorganic porous material divides into two parts: one is porous metals (such as porous Ni, Ti and stainless steel) [7,8], and the other is inorganic oxide ceramics (such as porous Al_2O_3) and non-oxide ceramics (such as porous SiC) [9,10]. Compared with porous metals, layered Ti_3AlC_2 ceramic has a better corrosion resistant performance in acid/alkali solution. And compared with conventional ceramics (such as porous

SiC, Al_2O_3), Ti_3AlC_2 ceramic can be easily machined by tools. Owing to its excellent corrosion resistance and machinability properties, it may replace current inorganic porous material in rugged environments. Furthermore, the tentative application of this material for separation and purification in CoSO_4 hydrometallurgy has yielded some useful results in Internet Technology Chendu Co., Ltd.

In the past two decades, Ti_3AlC_2 used as structural material has been fabricated through a variety of methods, including the spark plasma sintering (SPS) technique [11,12], hot-pressing technique [13], self-propagating high-temperature synthesis (SHS) [14], solid–liquid synthesis reaction and a simultaneous in-situ hot-pressing process technique [15]. Pietzka and Schuster first reported the synthesis of Ti_3AlC_2 by sintering cold-compacted powder mixtures of Ti, TiAl, Al_4C_3 and carbon at 1300 °C in H_2 atmosphere for 20 h [16]. Tzeonov and Barsoum first prepared bulk polycrystalline samples of Ti_3AlC_2 by reactively hot isostatically pressing (HIP) with a mixture of titanium, graphite, and Al_4C_3 powders at 1400 °C [3]. Zhou et al. fabricated high-purity Ti_3SiC_2 and Ti_3AlC_2 using the spark plasma sintering (SPS) technique with raw material of TiC, Ti, Si, and Al powders [11]. Łopaciński et al.

*Corresponding author. Tel.: +86 731 8836144; fax: +86 731 8710855.

E-mail address: yuehui@mail.csu.edu.cn (Y. He).

employed a direct combustion synthesis method to fabricate Ti_3AlC_2 with elemental Ti, Al, and C powders [17]. Wang et al. reported a novel solid–liquid reaction synthesis and simultaneous in-situ hot pressing process for the fabrication of fully dense Ti_3AlC_2 with high purity utilizing commercially available elemental powders of Ti, Al and graphite as initial materials [15]. Compared with the synthesis methods mentioned above, the spark plasma sintering (SPS) technique and hot-pressing (HP) technique are costly and difficult to apply in continuous production, while self-propagating high-temperature synthesis (SHS) is a thermal explosion reaction within several seconds, which is inapplicable for near-net-shape work-pieces. Reactive synthesis readily makes manufacture of samples with large size and complex shape possible. Besides it is also time-consuming and attains good properties with a lower temperature. Therefore, it is significant for promoting ceramics to be used in industry.

Although the fabrication of dense Ti_3AlC_2 with reactive synthesis technology have been published by many authors, but there is rare report about preparing porous Ti_3AlC_2 and even less about preparation without any pore former. We have successfully made porous Ti_3AlC_2 by using only TiH_2 , Al and graphite as raw materials through reaction synthesis and clearly depicted its pore structures and phase transformation in part of the Ti–Al–C system. Moreover, in conventional reaction synthesis method, a fast heating rate accompanied with in-situ hot-pressing process avoids the formation of pores. In this study, we demonstrate our success to fabricate porous Ti_3AlC_2 through the mixture composition in vacuum furnace with slow heating rate. The slow heating rate will ensure atom full diffusion to form vacancies and offset the uncontrollable compact shape made by SHS method with high heating rate and thermal explosion. The vacuum condition could avoid the influence of complicated environment with air atmosphere or pressure, which makes the investigation of pore evolution rule simpler. This work mainly focuses on the effect of Al content on phase constitution, pore structure, permeability, porosity, and the pore forming mechanism is also investigated.

2. Experimental procedure

All the work was conducted using powder mixtures of titanium hydride (99.7% pure, -400 mesh), Al (99.5% pure, -325 mesh) and graphite (99.8% pure, $5\text{--}6\text{ }\mu\text{m}$). Typically, the powder mixtures were ball-milled for 12 h with ZrO_2 ball/powder ratio of 1:1 (mass ratio). The raw powders were mixed by $\text{TiH}_2\text{:Al:C}$ with atomic ratios of $3\text{:}n\text{:}2$ (n is from 0.7 to 1.4 with an increment of 0.1) as starting material. Then, the starting materials and stearic acid were mixed and ball milled for 2 h in an ethanol solution. The ball-milled slurry was dried at $60\text{ }^\circ\text{C}$, and then pelletized and sieved through a -100 mesh. The dried mixtures were cold-pressed into green compacts under pressure of 200 MPa, with dimensions of $\varnothing 32\text{ mm} \times 2\text{ mm}$, and then sintered in a vacuum furnace with a vacuum of $2.0 \times 10^{-3}\text{ Pa}$. The sintering processes is illustrated in Fig. 1, in which four holding platforms were indicated. The first temperature holding platform was to remove the moisture in

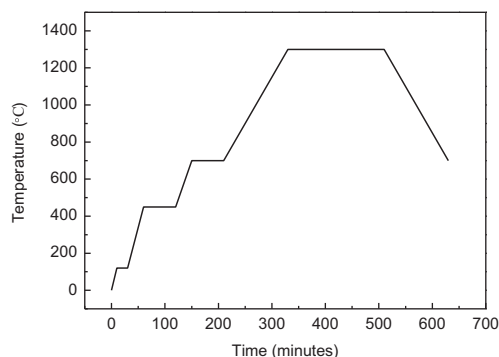


Fig. 1. The illustration of sintering procedure.

the vacuum furnace. The second platform was corresponding to the decomposition of stearic acid with temperature of $450\text{ }^\circ\text{C}$. The third platform was corresponding to the decomposition of titanium hydride with temperature of $700\text{ }^\circ\text{C}$. The last platform was corresponding to the formation of Ti_3AlC_2 with temperature of $1300\text{ }^\circ\text{C}$. The heating rate was less than $5\text{ }^\circ\text{C/min}$ during the whole process in order to preserve the original shape. The temperature deviation is $+10\text{ }^\circ\text{C}$.

The sintered samples with different Al contents were characterized by X-ray diffraction (XRD: Dmax 2500VB), with a scan rate of $4^\circ/\text{min}$ and a step size of 0.02° . The volumes of the disc were measured by vernier caliper before and after sintering to examine the generation of the volume expansion. The pore structure was characterized by scanning electron microscopy (SEM), and the open porosity and overall porosity were measured by the Archimedes' method. The pore size and permeability were measured by aperture measuring apparatus. The mechanism of pore size test is based on the bubble point method [18].

3. Results and discussion

3.1. Phase identification and reaction mechanism

Fig. 2 presents XRD diffractograms for mixtures of TiH_2 , Al and graphite powders with different Al contents after sintering at $1300\text{ }^\circ\text{C}$ for 3 h. The discs are composed of three phase constitutions (Ti_2AlC , TiC and Ti_3AlC_2) and very small amounts of the starting material (TiH_2 , Al and C) are detected, because they have reacted completely. When the content of aluminum is 0.7 (molar ratio in the mixtures), the main phase is TiC and Ti_2AlC , with low amounts of Ti_3AlC_2 . As Al content increases from 0.8 to 1.2, Ti_3AlC_2 becomes the main phase, and TiC becomes weaker and weaker. The TiC disappears and the pure Ti_3AlC_2 is observed as the content of Al attains 1.2 mol. Then the TiC appears again by increasing the amount of aluminum (when the Al content is more than 1.2 mol). These results illustrate that the pure porous Ti_3AlC_2 ceramics can be obtained by adjusting the amount of aluminum. Theoretically, pure Ti_3AlC_2 could be obtained with aluminum of 1 mol, whereas the aluminum of 1.2 mol is desired. The possible reason for that is the evaporation of aluminum at high temperature.

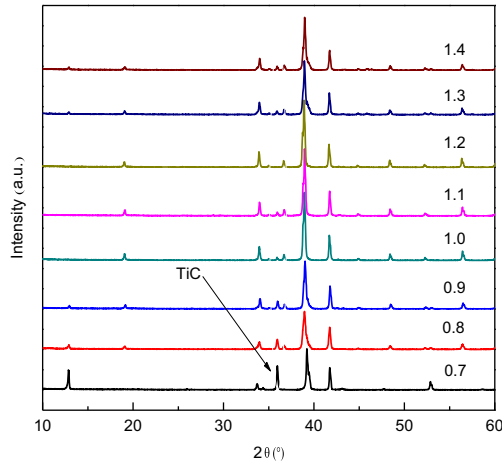


Fig. 2. X-ray diffractograms of porous Ti_3AlC_2 showing the effect of raw material composition on the final phase composition.

Table 1
The weight percentage of three phase constitution.

Al content	Phase constitution		
	Ti_3AlC_2	TiC	Ti_2AlC
0.7	0	86.87	13.13
0.8	84.99	8.39	6.62
0.9	87.04	10.89	2.07
1.0	93.24	3.76	0
1.1	95.91	4.09	0
1.2	100	0	0
1.3	92.74	5.70	1.56
1.4	93.34	5.22	1.44

In order to calculate the weight percents of Ti_3AlC_2 in sintered samples, the diffraction peaks of (104) peak of Ti_3AlC_2 , (111) peak of TiC and (002) peak of Ti_2AlC are detected. According to the reference of Peng et al. presented and PDF cards of Ti_3AlC_2 , the intensity of (002) peak is 0.27 that of (104) [19]. The calculated weight percentage of Ti_3AlC_2 , TiC and Ti_2AlC are listed as follows:

$$\begin{cases} w_a = \frac{0.27I_a}{0.27I_a + 0.220I_b + 0.084I_c} \\ w_c = \frac{I_c}{3.214I_a + 2.619I_b + I_c} \\ w_b = \frac{I_b}{1.227I_a + I_b + 0.382I_c} \end{cases} \quad (1)$$

where, w_a , w_b and w_c are the weight percent of Ti_3AlC_2 , Ti_2AlC and TiC. Similarly, the I_a , I_b and I_c stand for the intensities of the peaks of Ti_3AlC_2 , Ti_2AlC and TiC mentioned above. The calculated results are listed in Table 1.

The reaction mechanism for synthesis of porous Ti_3AlC_2 is investigated by thermodynamics calculation. The original parameters of TiAl, TiAl_3 and TiC are proposed by Barin and list in Table 2 [20], it is believed that TiC is very stable at high temperature. The formation of TiC from Ti and C is an exothermic reaction and Ti/C bonding is stronger than Ti/Al bonding. However, it is interesting to notice that TiAl compounds could be formed easily at 800 °C, it is because the reaction rate of

Table 2

Gibbs free formation enthalpies for Ti_3AlC_2 including the most competing phases.

Temperature	Most competing phases		
	TiAl (KJ mol^{-1})	TiAl_3 (KJ mol^{-1})	TiC (KJ mol^{-1})
1000 K	−68.185	−120.795	−173.115
1100 K	−66.357	−114.735	−172.021
1200 K	−64.378	−108.491	−170.773
1300 K	−62.165	−101.491	−169.81

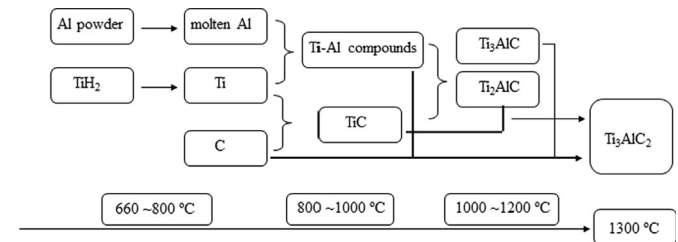


Fig. 3. The reaction route to synthesize Ti_3AlC_2 .

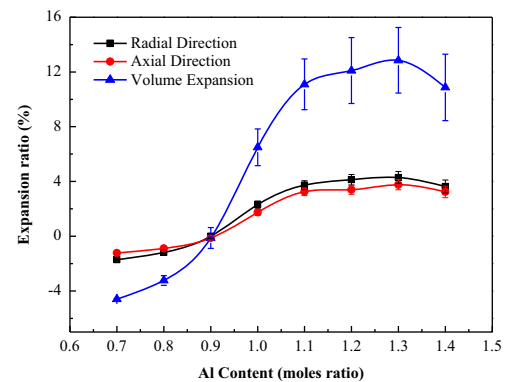


Fig. 4. The volume and dimension expansion of the compacts with Al content increasing from 0.7 to 1.4.

molten Al and Ti is higher than that of solid C and Ti. Another reason may be the wetting angle of molten Al and Ti is larger than that of C and Ti. As the temperature increases from 800 °C to 1000 °C, redundant Ti reacts with C to form TiC, and the new-formed TiC are surrounded by Ti–Al compounds, as a result, TiC react with Ti–Al compounds directly to form Ti_2AlC . With sintering temperature increasing from 1000 °C to 1300 °C, the final product Ti_3AlC_2 is synthesized. The reaction route to synthesize Ti_3AlC_2 is expressed in Fig. 3.

3.2. Effect of Al content on volume evolution

Fig. 4 shows the volume and dimension expansion ratios alteration with Al content increasing (the ratio is the volume and dimension increment of diameter and height after sintering divided by that of green compacts). As illustrated in Fig. 4, with Al content increasing from 0.7 to 1.1, the volume expansions increase from −4.59% to 11.09% sharply. After that, with Al content increasing from 1.1 to 1.3, the volume expansions increase from 11.09% to 12.85% slowly. And it is interesting

that the volume expansion began to reduce to 10.87% with Al content of 1.4. The volume expansion developing route may be due to the formation of Ti_3AlC_2 , and the volume expansion reduction with Al content of 1.4 is mainly due to the existence of excessive Al metal in the system. As the sintering temperature exceeds the melting point of Al, the excessive Al metal will melt, which may result in the shrinkage of the sintered grains due to the surface tension of liquid phase [18]. Besides, Al melt will fill to pores leading to porosity reduction, and Al evaporation leading to the pore size increment, which will be discussed in Section 3.3.

In order to investigate the relationship between the volume expansion and the open porosity, Jiang et al. have investigated the mathematical relationship between volume expansion and the open porosity [18]. The expression can be expressed as

$$\theta_p = -\frac{\rho_0(1-\theta_0)}{\rho} \frac{1}{1+\alpha} + (1-\theta_c) \quad (2)$$

where ρ_0 and ρ are the theoretical densities of the compact before and after the sintering, θ_0 is the initial overall porosity in green compacts, θ_p is the open porosity after the sintering, α is the volume expansion ratio, and θ_c is the closed porosity in sintered compact. Since the open porosity decreases when Al content is beyond 1.2 (molar ratio), the composition of Al content below $\text{Ti}_3\text{AlC}_{1.2}$ is considered. To investigate the relationship between the volume expansion and open porosity, the θ_p is used as the Y-axis and $1/(1+\alpha)$ as the X-axis by drawing standard curve, and the experimental data is shown in Fig. 5. The sensational linear relationship between θ_p and $1/(1+\alpha)$ has been verified when the Al content below 1.2.

3.3. Porous characteristics of sintered samples with increasing Al additions

The pore structure parameters are important for porous Ti_3AlC_2 ceramics in practical application. Therefore, it is significant to understand the effect of Al content on pore structural variation. The open porosity, overall porosity, open pore proportion, the maximum pore size, the average pore size and permeability evolution route with increasing aluminum amount are investigated systematically.

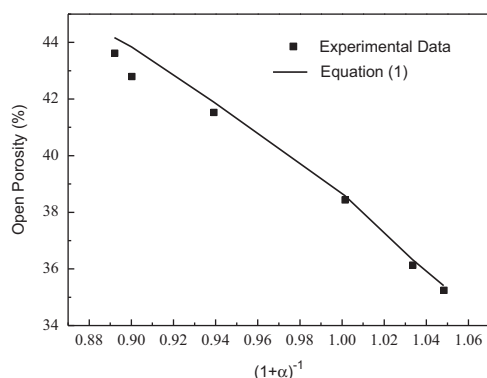


Fig. 5. Relation between the open porosity and volume expansion as theoretically calculated and experimentally observed.

Fig. 6(a) shows the overall porosity, open porosity and the open porosity proportion of the porous Ti_3AlC_2 ceramics as a function of the Al content. It can be seen that with the increasing amount of aluminum (from 0.7 to 1.2), the open porosity increases from 35.25% to 43.62%, and the overall porosity increases from 37.10% to 47.23%. A similar curve is obtained with the relationship between the weight percentage of Ti_3AlC_2 and the Al content. The results indicate that with the increasing weight percentage of Ti_3AlC_2 , the porosity increases as well, and the maximum porosity is observed at aluminum content of 1.2 mol.

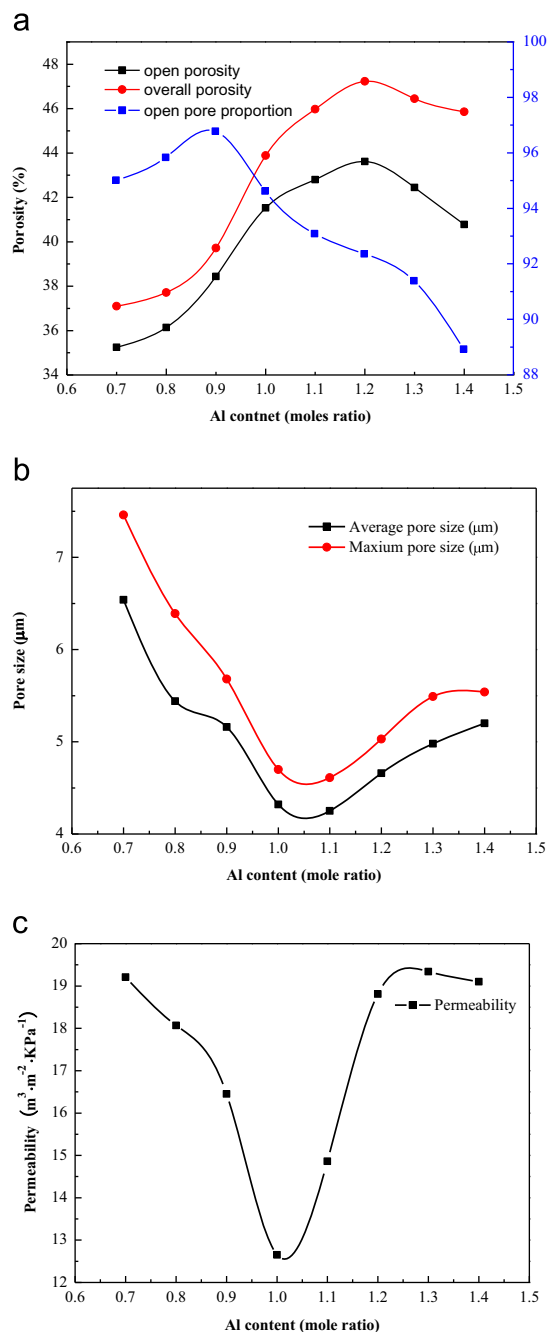


Fig. 6. The pore structures of porous Ti_3AlC_2 ceramics as a function of the Al contents (a) overall porosity, open porosity and the open porosity proportion, (b) maximum pore size and average pore size, and (c) permeability.

Fig. 6(b) shows the maximum pore size and average pore size of the porous Ti_3AlC_2 ceramics as a function of the Al content. It is interesting to notice that the pore size evolution rule is opposed to that of permeability, with the Al content varying from 0.7 to 1.0, the pore size decreases apparently during this stage. However, when Al content increases from 1.1 to 1.2, the pore size keeps stable with the increasing Al content. As the Al content increases continuously from 1.2 to 1.4, the pore size increases dramatically.

Fig. 6(c) shows the permeability variation of the porous Ti_3AlC_2 ceramics with Al content increasing. It can be seen that the changing tendency is similar with the effect of aluminum content on pore size. The permeability monotonically decreases with Al content increasing from 0.7 to 1.0, and after that, the permeability increases sharply with the increasing amount of aluminum content (from $12.65 \text{ m}^3 \text{ m}^{-2} \text{ kPa}^{-1} \text{ h}^{-1}$ with the Al content of 1.0 to $18.81 \text{ m}^3 \text{ m}^{-2} \text{ kPa}^{-1} \text{ h}^{-1}$ with the Al content of 1.2). With aluminum content increasing from 1.3 to 1.4, the permeability changes smoothly.

3.4. Pore forming mechanism

In order to explain the pore structure variation accompanied with aluminum content, a possible reaction mechanism is proposed. It is necessary to notice that the open porosity and overall porosity increases with the amount of Ti_3AlC_2 increasing. However, the evolution route of average pore size, maximum pore size and permeability is opposite to that of Ti_3AlC_2 , which means that the pore structure evolution is depend on the phase transformation process.

With the purpose of investigating the phase transformation process on synthesis of porous Ti_3AlC_2 , $\text{TiH}_2/\text{Al}/\text{TiC}$ powders with atomic ratio of 3:1.2:2 were selected to investigate the pore structure forming process. The green compacts were heating from 800°C to 1300°C , and XRD pattern was employed to detect the phase constitution. Fig. 7(a) shows the XRD patterns of the samples sintered at different temperatures. At 800°C , five phases (Ti, C, Ti_3Al , TiAl , and TiAl_2) coexist. It means that with sintering temperature at 800°C , TiH_2 has de-composited completely, and molten Al reacts with

Ti preferentially. He et al. has reported a method to fabricate Ti–Al micro/nanometer-sized porous alloys by the Kirkendall effect [21]. They believed that the pores are produced by great diffusion-rate discrepancies between Ti and Al in the alloy system, with reacting of Ti and Al into Ti–Al compound, the net movement and consumption of Al element will result in a large number of pores near the original positions of Al atoms. And the higher the Al content increases, the larger is the pore size. However, when the Al content varied from 30 wt% to 40 wt% (calculated as atomic ratio, the Ti: Al varies from 1:0.76 to 1:1.18), the pore size almost remains constant [18], which is also proved by the little variation of permeability.

Fig. 7(b) shows the XRD patterns of the samples sintered at 1000°C , and six phases (C, Ti_3Al , TiC , TiAl , Ti_3AlC and Ti_2AlC) coexist. Li et al. proposed a model for formation of a single-phase Ti_3AlC_2 from a mixture of Ti, Al and TiC powders with Sn as an additive [22]. They believed that when sintering temperature is above 650°C , Al melts and reacts with Ti to form intermediate Ti–Al compounds, that are Ti_2Al , TiAl_3 , TiAl_2 and TiAl in sequence in the Ti/Al/TiC/0.1Sn sample. With heating temperature increasing gradually, superfluous Ti and C reacted to turn into TiC. With enough Ti–Al compounds and TiC in the reaction system, both Ti_2AlC and Ti_3AlC_2 should be synthesized at certain temperature. The reaction process may illustrate that as heating temperature increases, a reaction at the interface between Ti and graphite particles starts to occur and compose of a thin layer of TiC. Then, the thin layer of TiC would dissolve/diffuse into the Ti–Al alloys. With more and more TiC diffusing into the Ti–Al alloys, TiC will deviate from its original position and the pores will be formed. At the same time, Ti–Al compounds react with TiC to synthesize Ti_3AlC and Ti_2AlC . The volume of original Ti–Al compounds will be expands, and they will extrude the pores so that the pores are oppressed. In general, the overall effect of the pores produced by TiC diffusing into the Ti–Al alloys and pores constricted by volume expansion of Ti–Al compounds guarantees the sample large porosity together with small pore size. Therefore, with more TiC dissolve, the smaller the pore size is and the higher the porosity is. The results also explain the reason why the pore size decreases with Al content increasing, while the porosity increases with Al content increasing. As is shown in Table 1, with the content of Al increases from 0.7 to 1.2, the amount of TiC decreases gradually. It reveals that when TiC will dissolves into Ti–Al compounds with Al content increasing, the pore size decreases and porosity increases step by step. With Al content increasing continuously, the amount of TiC decreases gradually, and the pore size increases and porosity decreases again. As the results show that, the permeability firstly decreases, and then increases with increasing Al content. This may attribute to the combined effect of TiC escaping from its original position and TiC dissolving/diffusing into Ti–Al compounds. When diffusion effect plays a leading role, the permeability will be decreased, and vice versa.

Fig. 8 shows the SEM images of porous Ti_3AlC_2 with aluminum of 1.2, it can be seen that porous Ti_3AlC_2 is well developed and morphology is layer-shaped structure.

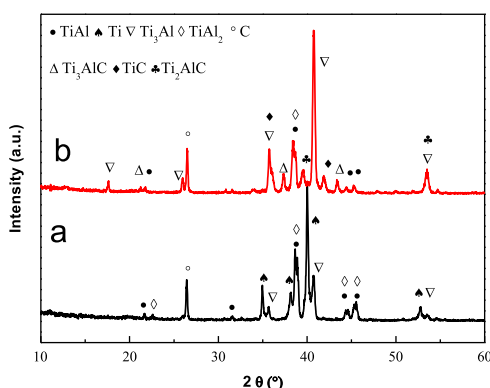


Fig. 7. XRD patterns of synthesized samples with different sintering temperature and holding for 3 h. (a) 800°C , and (b) 1000°C .

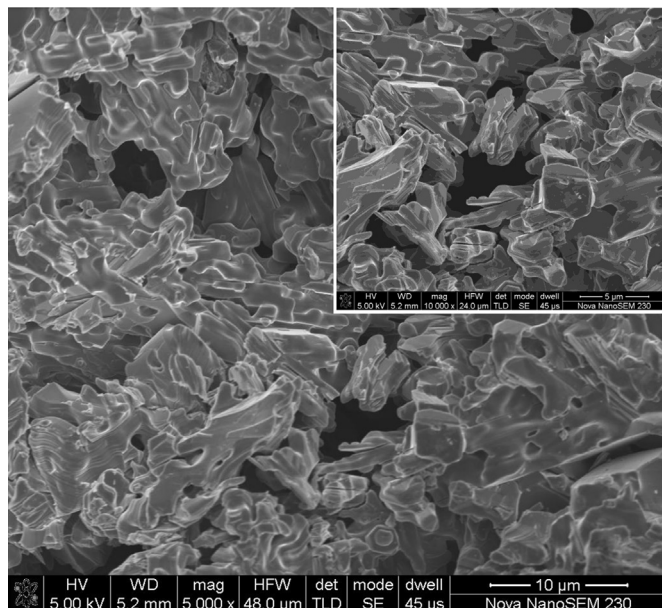


Fig. 8. The SEM images of porous Ti_3AlC_2 .

4. Conclusions

Porous Ti_3AlC_2 ceramics with Al content ranging from 0.7 to 1.4 (atomic ratio) were successfully fabricated by the reactive synthesis of TiH_2 , Al and graphite. With increasing amount of Al content, the sintered samples have three typical phases: Ti_2AlC , TiC and Ti_3AlC_2 . And pure Ti_3AlC_2 phase was obtained with TiH_2 :Al:C of 3:1.2:2. The effects of Al content on pore structures were investigated systematically, which reveals that the open porosity and overall porosity increased with Al content increasing, while the pore size and permeability changed in contrast with Al content. The pore structure variation tendency, to some extent, related to the amount of Ti_3AlC_2 phase in the final products. The phase transition process and pore forming mechanism were also investigated.

Acknowledgments

This project is financially supported by the Natural Science Foundation of China (51071178, 50721003 and 50825102), Hunan Provincial Natural Science Foundation of China (05JJ30097) and State Science and Technology support program (2012BAC02B05).

References

[1] X.H. Wang, Y.C. Zhou, Layered machinable and electrically conductive Ti_2AlC and Ti_3AlC_2 ceramics: a review, *Journal of Materials Science and Technology* 26 (2010) 385–416.

[2] A. Zhou, C.-A. Wang, Z. Ge, L. Wu, Preparation of Ti_3AlC_2 and Ti_2AlC by self-propagating high-temperature synthesis, *Journal of Materials Science Letters* 20 (2001) 1971–1973.

[3] N.V. Tzenov, M.W. Barsoum, Synthesis and characterization of Ti_3AlC_2 , *Journal of the American Ceramic Society* 83 (2000) 825–832.

[4] J. Zhu, B. Mei, J. Liu, X. Xu, Synthesis of high-purity Ti_3SiC_2 and Ti_3AlC_2 by hot-pressing (HP), *Journal of Materials Science Letters* 22 (2003) 1111–1112.

[5] D. Li, Y. Liang, X. Liu, Y. Zhou, Corrosion behavior of Ti_3AlC_2 in NaOH and H_2SO_4 , *Journal of the European Ceramic Society* 30 (2010) 3227–3234.

[6] Z. Lin, Y. Zhou, M. Li, J. Wang, Hot corrosion and protection of Ti_2AlC against Na_2SO_4 salt in air, *Journal of the European Ceramic Society* 26 (2006) 3871–3879.

[7] C. Wen, M. Mabuchi, Y. Yamada, K. Shimojima, Y. Chino, T. Asahina, Processing of biocompatible porous Ti and Mg, *Scripta Materialia* 45 (2001) 1147–1153.

[8] B. Li, L. Rong, Y.-Y. Li, V. Gjunter, Synthesis of porous Ni–Ti shape-memory alloys by self-propagating high-temperature synthesis: reaction mechanism and anisotropy in pore structure, *Acta Materialia* 48 (2000) 3895–3904.

[9] S. Zhu, S. Ding, H.a. Xi, R. Wang, Low-temperature fabrication of porous SiC ceramics by preceramic polymer reaction bonding, *Materials Letters* 59 (2005) 595–597.

[10] J. Cao, C. Rambo, H. Sieber, Preparation of porous Al_2O_3 -ceramics by biotemplating of wood, *Journal of Porous Materials* 11 (2004) 163–172.

[11] W. Zhou, B. Mei, J. Zhu, X. Hong, Synthesis of high-purity Ti_3SiC_2 and Ti_3AlC_2 by spark plasma sintering (SPS) technique, *Journal of Materials Science* 40 (2005) 2099–2100.

[12] W. Zhou, B. Mei, J. Zhu, X. Hong, Rapid synthesis of Ti_2AlC by spark plasma sintering technique, *Materials Letters* 59 (2005) 131–134.

[13] J.-H. Han, S.-S. Hwang, D. Lee, S.-W. Park, Synthesis and mechanical properties of Ti_3AlC_2 by hot pressing TiC/Al powder mixture, *Journal of the European Ceramic Society* 28 (2008) 979–988.

[14] X. He, X. Qian, Y. Sun, Y. Li, C. Zhu, Y. Zhou, Self-propagating high temperature synthesis of intragranular TiC – Ti_3AlC_2 composites, *Advances in Applied Ceramics* 109 (2010) 338–340.

[15] X. Wang, Y. Zhou, Microstructure and properties of Ti_3AlC_2 prepared by the solid–liquid reaction synthesis and simultaneous in-situ hot pressing process, *Acta Materialia* 50 (2002) 3143–3151.

[16] M. Pietzka, J. Schuster, The ternary boundary phases of the quaternary system Ti–Al–CN, in: *Proceedings of the Concerted Action on Materials Science, Part A*, Leuven, 1992.

[17] M. Łopaciński, J. Puszynski, J. Lis, Synthesis of ternary titanium aluminum carbides using self-propagating high-temperature synthesis technique, *Journal of the American Ceramic Society* 84 (2001) 3051–3053.

[18] Y. Jiang, Y. He, N. Xu, J. Zou, B. Huang, C. Liu, Effects of the Al content on pore structures of porous Ti–Al alloys, *Intermetallics* 16 (2008) 327–332.

[19] C. Peng, C.-A. Wang, Y. Song, Y. Huang, A novel simple method to stably synthesize Ti_3AlC_2 powder with high purity, *Materials Science and Engineering: A* 428 (2006) 54–58.

[20] I. Barin, F. Sauert, E. Schultze-Rhnhof, W.S. Sheng, *Thermochemical Data of Pure Substances*, VCH, Weinheim, Germany, 1993.

[21] Y. He, Y. Jiang, N. Xu, J. Zou, B. Huang, C.T. Liu, P.K. Liaw, Fabrication of Ti–Al micro/nanometer-sized porous alloys through the Kirkendall effect, *Advanced Materials* 19 (2007) 2102–2106.

[22] S. Li, W. Xiang, H. Zhai, Y. Zhou, C. Li, Z. Zhang, Formation of a single-phase Ti_3AlC_2 from a mixture of Ti, Al and TiC powders with Sn as an additive, *Materials Research Bulletin* 43 (2008) 2092–2099.